Disappearance of nuclear deformation in hypernuclei: A perspective from a beyond-mean-field study

著者	H Mei, K Hagino, J M Yao, T Motoba
journal or publication title	Physical Review C
volume	97
number	064318
page range	1-6
year	2018-06-25
URL	http://hdl.handle.net/10097/00125386

doi: 10.1103/PhysRevC.97.064318

Disappearance of nuclear deformation in hypernuclei: A perspective from a beyond-mean-field study

H. Mei,[1] K. Hagino,[1,2] J. M. Yao,[3,4] and T. Motoba[5,6]

[1]*Department of Physics, Tohoku University, Sendai 980-8578, Japan*
[2]*Research Center for Electron Photon Science, Tohoku University, 1-2-1 Mikamine, Sendai 982-0826, Japan*
[3]*FRIB/NSCL Laboratory, Michigan State University, East Lansing, Michigan 48824, USA*
[4]*School of Physical Science and Technology, Southwest University, Chongqing 400715, China*
[5]*Laboratory of Physics, Osaka Electro-Communications University, Neyagawa 572-8530, Japan*
[6]*Yukawa Institute for Theoretical Physics, Kyoto University, Kyoto 606-8502, Japan*

(Received 18 April 2018; revised manuscript received 25 May 2018; published 25 June 2018)

The previous mean-field calculation [Phys. Rev. C **78**, 054311 (2008)] has shown that the oblate deformation in ^{28,30,32}Si disappears when a Λ particle is added to these nuclei. Here, we investigate this phenomenon by taking into account the effects beyond the mean-field approximation. To this end, we employ the microscopic particle-rotor model based on the covariant density functional theory. We show that the deformation of ^{30}Si does not completely disappear, even though it is somewhat reduced, after a Λ particle is added if the beyond-mean-field effect is taken into account. We also discuss the impurity effect of a Λ particle on the electric-quadrupole transition and show that an addition of a Λ particle leads to a reduction in the $B(E2)$ value, as a consequence of the reduction in the deformation parameter.

DOI: 10.1103/PhysRevC.97.064318

I. INTRODUCTION

The nuclear deformation is one of the most important concepts in nuclear physics [1,2]. Whereas only those states with good angular momentum are realized in the laboratory, atomic nuclei can be deformed in the intrinsic frame, in which the rotational symmetry is spontaneously broken. This idea nicely explains the existence of rotational bands as well as enhanced electric transitions within the rotational bands in many nuclei. Theoretically, the nuclear deformation is intimately related to the mean-field approximation [2,3], but there have also been recent attempts to describe the characteristics of deformed nuclei by using symmetry-preserved frameworks [4–8].

In this paper, we discuss the nuclear deformation of single-Λ hypernuclei [9–21], where a Λ particle is added to atomic nuclei. See Refs. [22–24] for reviews on hypernuclei. A characteristic feature of hypernuclei is that a Λ particle does not suffer from the Pauli principle of nucleons, and thus its wave function can have a large probability at the center of hypernuclei. This may significantly affect the structure of atomic nuclei.

In the history of hypernuclear studies, when the experimental data of strangeness-exchange (K^-,π^-) reactions came out from CERN, Feshbach proposed the concept of "shape polarizability;" that is, a possible change of nuclear radius and deformation induced by the hyperon participation [9]. Subsequently, Žofka carried out Hartee–Fock calculations for hypernuclei to analyze such effects on even-even nuclei with $Z = N$ and $A < 40$ [10]. He found that the relative change in quadrupole deformation should be maximum at $^{9}_{\Lambda}$Be and $^{29}_{\Lambda}$Si in the p shell and sd shell, respectively, although the expected change was not so large (only of the order of 1%–4% in the sd shell). See also Ref. [11]. In modern light of nuclear structure studies, however, such response to the Λ participation depends sensitively on the nuclear properties such as softness and potential shape. As a matter of fact, based on the relativistic mean-field (RMF) theory, it was argued that the nuclear deformation may disappear in some nuclei, such as ^{12}C and ^{28,30,32}Si, when a Λ particle is added to these nuclei [12]. That is, those deformed nuclei turn out to be spherical hypernuclei after a Λ particle is put in them. See also Refs. [14,15] for a similar conclusion. It has been shown that a softness of the potential-energy surface in the deformation space is a primary cause of this phenomenon [13].

In general, one expects a large fluctuation around the minimum when a potential surface is soft against deformation. This effect can actually be taken into account by going beyond the mean-field approximation with the generator coordinate method (GCM) [2,3]. In addition, one can also apply the angular momentum and the particle-number projections to a mean-field wave function, in which these symmetries are spontaneously broken. Such calculations have been performed recently not only for ordinary nuclei [25–31] but also for hypernuclei [32–34]. Here, we apply the beyond-mean-field calculations to a typical soft hypernucleus as the most appropriate theoretical treatment for the dynamical shape fluctuation.

The aim of this paper is then to assess the effect beyond the mean-field approximation on the phenomenon of disappearance of nuclear deformation, which takes place in hypernuclei whose potential surface is soft. A similar work has been carried out with the antisymmetrized molecular dynamics [35]. Here, we instead employ the microscopic particle-rotor model based on the covariant density functional theory [36–40], in which the Λ-particle motion is coupled to the core wave functions described with the beyond-mean-field method.

The paper is organized as follows: In Sec. II, we briefly summarize the microscopic particle-rotor model. In Sec. III, we apply this framework to the $^{31}_{\Lambda}$Si hypernucleus, for which the disappearance of deformation has been found in the mean-field approximation, and discuss the impurity effect of Λ particles on the structure of the soft nucleus, ^{30}Si. We then summarize the paper in Sec. IV.

II. MICROSCOPIC PARTICLE-ROTOR MODEL

We consider in this paper a single-Λ hypernucleus. The Hamiltonian for this system reads

$$H = T_\Lambda + H_{\rm core} + \sum_{i=1}^{A_C} v_{N\Lambda}(\boldsymbol{r}_\Lambda,\boldsymbol{r}_i), \tag{1}$$

where T_Λ is the kinetic energy of the Λ particle and $H_{\rm core}$ is the many-body Hamiltonian for the core nucleus, whose mass number is A_C. $v_{N\Lambda}(\boldsymbol{r}_\Lambda,\boldsymbol{r}_i)$ is the nucleon-Λ ($N\Lambda$) interaction, in which $\boldsymbol{r}_\Lambda$ and $\boldsymbol{r}_i$ denote the coordinates of the Λ particle and of the nucleons, respectively.

In the microscopic particle-rotor model, the total wave function for the system is described as

$$\begin{aligned}&\Psi_{JM_J}(\boldsymbol{r}_\Lambda,\{\boldsymbol{r}_i\})\\ &\quad= \sum_{j,l}\sum_{n,I}\mathcal{R}_{jlnI}(r_\Lambda)[\mathcal{Y}_{jl}(\hat{\boldsymbol{r}}_\Lambda)\otimes\Phi_{nI}(\{\boldsymbol{r}_i\})]^{(JM_J)}, \end{aligned}\tag{2}$$

where J is the angular momentum of the hypernucleus and M_J is its z component in the laboratory frame. $\mathcal{R}_{jlnI}(r_\Lambda)$ and $\mathcal{Y}_{jlm_j}(\hat{\boldsymbol{r}}_\Lambda)$ are the radial and the spin-angular wave functions for the Λ particle, with j, m_j, and l being the total single-particle momentum and its z component, and the orbital angular momentum, respectively. In Eq. (2), $\Phi_{nIM}(\{\boldsymbol{r}_i\})$ is a many-body wave function for the core nucleus, satisfying $H_{\rm core}|\Phi_{nIM}\rangle = \epsilon_{nI}|\Phi_{nIM}\rangle$, where I and M are the total angular momentum and its z component in the laboratory frame for the core nucleus, and n is the index to distinguish different states with the same I and M.

The radial wave function, $\mathcal{R}_{jlnI}(r_\Lambda)$, in Eq. (2) is obtained by solving the coupled-channels equations given by

$$0 = \langle[\mathcal{Y}_{jl}(\hat{\boldsymbol{r}}_\Lambda)\otimes\Phi_{nI}(\{\boldsymbol{r}_i\})]^{(JM_J)}|H - E_J|\Psi_{JM_J}\rangle \tag{3}$$

$$\begin{aligned}&= [T_\Lambda(jl)+\epsilon_{nI} - E_J]\mathcal{R}_{jlnI}(r_\Lambda)\\ &\quad+\sum_{j',l'}\sum_{n',I'}V_{jlnI,j'l'n'I'}(r_\Lambda)\,\mathcal{R}_{j'l'n'I'}(r_\Lambda),\end{aligned}\tag{4}$$

with

$$V_{jlnI,j'l'n'I'}(r_\Lambda) = \langle jlnI|\sum_{i=1}^{A_C} v_{N\Lambda}(\boldsymbol{r}_\Lambda,\boldsymbol{r}_i)|j'l'n'I'\rangle, \tag{5}$$

where $|jlnI\rangle \equiv |[\mathcal{Y}_{jl}(\hat{\boldsymbol{r}}_\Lambda)\otimes\Phi_{nI}(\{\boldsymbol{r}_i\})]^{(JM_J)}\rangle$.

In the microscopic particle-rotor model, the core wave functions Φ_{nIM} are constructed with the generator coordinate method by superposing projected Slater determinants $|\phi_{IM}(\beta)\rangle$ as

$$|\Phi_{nIM}\rangle = \int d\beta\, f_{nI}(\beta)|\phi_{IM}(\beta)\rangle, \tag{6}$$

where β is the quadrupole deformation parameter and $f_{nI}(\beta)$ is the weight function. In writing this equation, for simplicity, we have assumed that the core nucleus has an axially symmetric shape. Here, $|\phi_{IM}(\beta)\rangle$ is constructed as

$$|\phi_{IM}(\beta)\rangle = \hat{P}^I_{M0}\hat{P}^N\hat{P}^Z|\beta\rangle, \tag{7}$$

where $|\beta\rangle$ is the wave function obtained with a constrained mean-field method at the deformation β, and $\hat{P}^I_{M0}$, $\hat{P}^N$, and $\hat{P}^Z$ are the operators for the angular-momentum projection, the particle-number projection for neutrons, and that for protons, respectively. Notice that the K quantum number is zero in $\hat{P}^I_{M0}$ because of the axial symmetry of the wave function, $|\beta\rangle$. The weight function $f_{nI}(\beta)$ in Eq. (6) is determined by using the variational principle, which leads to the Hill–Wheeler equation [2],

$$\begin{aligned}&\int d\beta'\,[\langle\phi_{IM}(\beta)|H_{\rm core}|\phi_{IM}(\beta')\rangle\\ &\quad-\epsilon_{nI}\langle\phi_{IM}(\beta)|\phi_{IM}(\beta')\rangle]f_{nI}(\beta') = 0.\end{aligned}\tag{8}$$

Notice that, by setting $f_{nI}(\beta) = \delta(\beta-\beta_0)$ in Eq. (6), one can also obtain the projected energy surface $E_J(\beta_0)$ after solving the coupled-channels equations (4) [37]. (In this case, there is only one single state, $n = 1$, in the core nucleus for each I.)

See Refs. [36–40] for more details on the framework of the microscopic particle-rotor model.

III. DEFORMATION OF THE $^{31}_{\Lambda}$Si HYPERNUCLEUS

We now apply the microscopic particle-rotor model to $^{31}_{\Lambda}$Si as a typical example of hypernuclei which show the disappearance of nuclear deformation in the mean-field approximation. To this end, we employ the relativistic point-coupling model. For the core nucleus, ^{30}Si, we use the PC-F1 [41] parameter set, while we use PCY-S4 [42] for the $N\Lambda$ interaction. As we have shown in Ref. [39], the dependence of the results on the choice of the $N\Lambda$ interaction would not be large and the conclusion of the paper will remain the same, at least qualitatively, even if we use another set of the PCY-S interaction. The pairing correlation among the nucleons in the core nucleus is taken into account in the BCS approximation with a contact pairing interaction with a smooth energy cutoff, as described in Ref. [43]. We generate the reference states $|\beta\rangle$ in Eq. (7) by expanding the single-particle wave functions on a harmonic-oscillator basis with 10 major shells. The coupled-channels calculations are also solved by expanding the radial wave functions $\mathcal{R}_{jlnI}(r_\Lambda)$ on the spherical harmonic-oscillator basis with 18 major shells. In the coupled-channels calculations, we include the core states up to $n_{\rm max} = 2$ and $I_{\rm max} = 6$.

We first discuss the results for the core nucleus, ^{30}Si. Figure 1 shows the potential-energy curves for ^{30}Si as a function of the deformation parameter, β. The energy curve in the mean-field approximation shows a shallow minimum at $\beta = -0.22$ (see dotted line), which is similar to the energy curve for ^{28}Si shown in Ref. [12] obtained with the RMF theory with the meson-exchange NLSH parameter set [45].

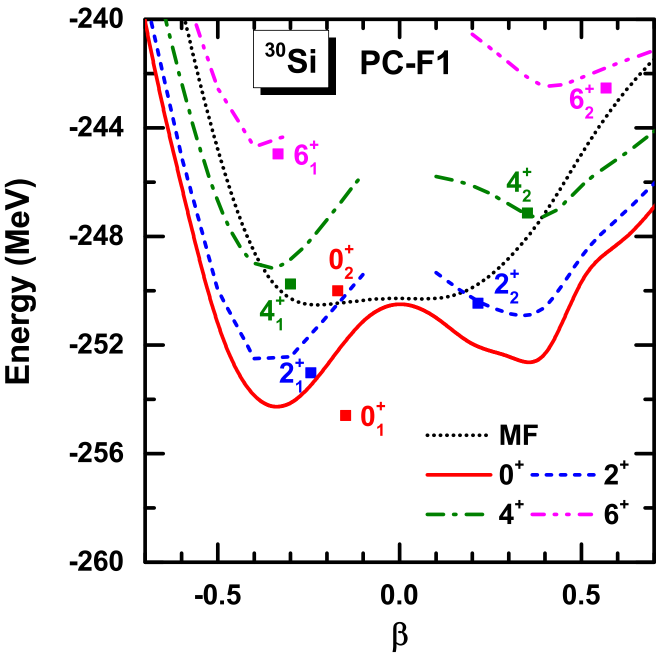

FIG. 1. The projected energy curves for the ^{30}Si nucleus as a function of the quadrupole deformation parameter β. The mean-field energy curves are shown by the dotted lines for comparison. The filled squares indicate the energy of the GCM solutions, which are plotted at their average deformation.

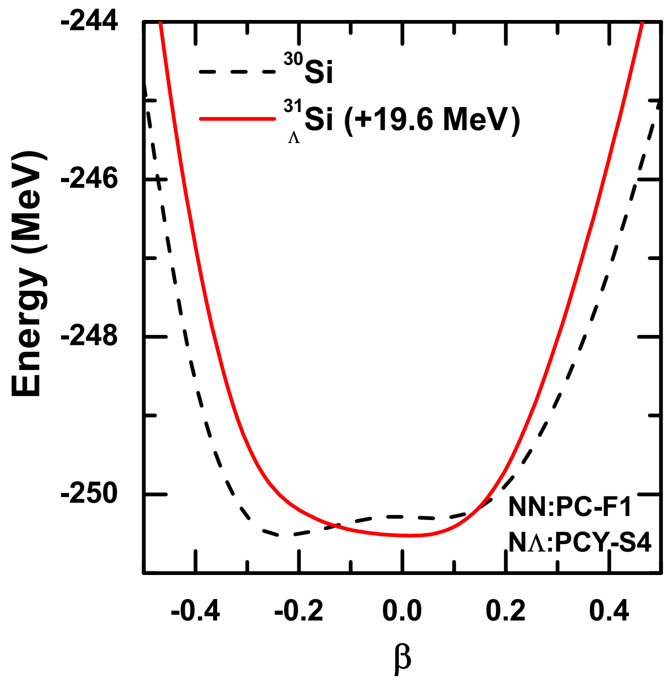

FIG. 3. The potential-energy curves in the mean-field approximation for the ^{30}Si nucleus (the dotted line) and for the $^{31}_{\Lambda}$Si hypernucleus (the solid lines). The energy curve for $^{31}_{\Lambda}$Si is shifted in energy as indicated in the figure to compare with that for ^{30}Si.

For the projected energy curves, this calculation yields a well-pronounced oblate minimum. For instance, for the 0^+ configuration, the minimum appears at $\beta = -0.35$. The results of the GCM calculations for the spectrum as well as the $E2$ transition probabilities are shown in Fig. 2. The energy of each state is plotted also in Fig. 1, at the position of the mean deformation for each state. These calculations reproduce the experimental data reasonably well, even though the $B(E2)$ values for the intraband and the interband transitions are somewhat overestimated and underestimated, respectively.

Let us now put a Λ particle onto the ^{30}Si nucleus and discuss the structure of the $^{31}_{\Lambda}$Si hypernucleus. Figure 3 shows the potential-energy surface in the mean-field approximation, in which the curve for the hypernucleus (the solid line) is shifted in energy as indicated in the figure so that the energy of the absolute minima becomes the same as that for the core nucleus (the dotted line). One can see that the potential minimum is shifted from the oblate shape to the spherical shape by adding a Λ particle to ^{30}Si. As we have mentioned, the same phenomenon has been found also with another relativistic interaction; that is, the the meson-exchange NLSH interaction [12]. Our interest in this paper is to investigate how this phenomenon is modified when the effect beyond the mean-field approximation is taken into account.

Figure 4 shows the projected energy curve, which includes the beyond-mean-field effect. The solid line shows the energy for the $1/2^+$ configuration of the $^{31}_{\Lambda}$Si hypernucleus. One notices that the energy at the spherical configuration is lowered when a Λ particle is added, as has also been indicated in the previous mean-field calculations (see also Fig. 3) [12,13]. Moreover, the deformation at the energy minimum is shifted towards the spherical configuration; that is, from $\beta = -0.35$ to $\beta = -0.30$. Even though care must be taken in interpreting the projected energy surface, which includes only the rotational correction to the mean-field approximation while the vibrational correction is left out [46], this may indicate that the collectivity is somewhat reduced in the hypernucleus.

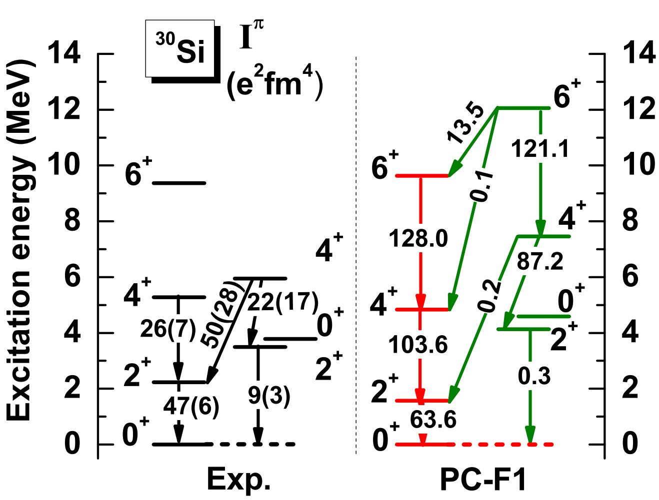

FIG. 2. The low-lying spectrum of the ^{30}Si nucleus obtained with the GCM method with the covariant density functional with the PC-F1 set. The arrows indicate the electric-quadrupole ($E2$) transition strengths, plotted in units of e^2 fm^4. These are compared with the experimental data taken from Ref. [44].

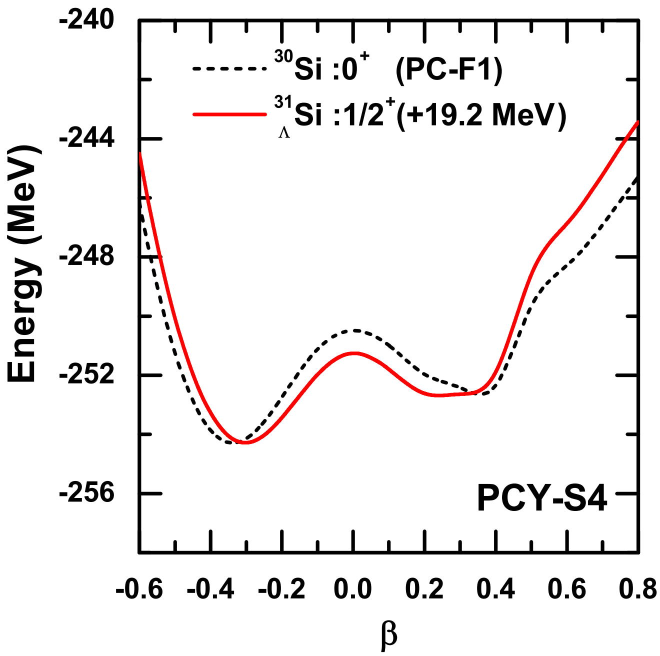

FIG. 4. The projected energy curve for the $J^\pi = 1/2^+$ configuration of the $^{31}_{\Lambda}$Si hypernucleus (the solid lines). This is shifted in energy as indicated in the figure to compare with the energy curve for the core nucleus, ^{30}Si (the dotted lines).

To gain a deeper insight into the effect of Λ particle on the collectivity of the hypernucleus, Fig. 5 shows the spectrum of $^{31}_{\Lambda}$Si for the positive-parity states obtained with the microscopic particle-rotor model. One can observe that the spectrum resembles that in the core nucleus shown in Fig. 2. These positive-parity states are in fact dominated by the Λ hyperon in the s orbit coupled to the positive-parity states of the core nucleus. However, if one takes the ratio of

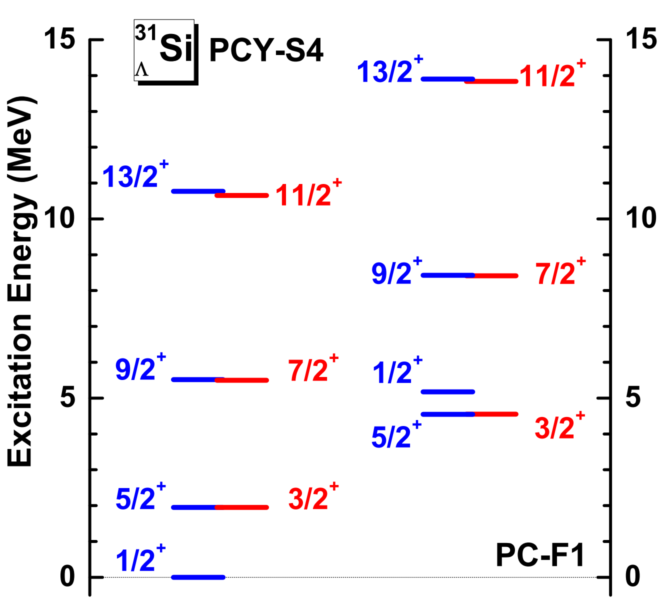

FIG. 5. The low-lying spectrum for positive-parity states of the $^{31}_{\Lambda}$Si hypernucleus obtained with the microscopic particle-rotor model.

TABLE I. The $E2$ transition strengths (in units of e^2 fm^4) for low-lying positive-parity states of ^{30}Si and $^{31}_{\Lambda}$Si obtained with the PC-F1 parameter set for the NN interaction. The c$B(E2)$ values denote the corresponding $B(E2)$ values for the core transition in the hypernucleus, defined by Eq. (9). The changes in the $B(E2)$ is indicated with the quantity defined by $\Delta \equiv [cB(E2) - B(E2;{}^{30}\mathrm{Si})]/B(E2;{}^{30}\mathrm{Si})$.

^{30}Si		$^{31}_{\Lambda}$Si			
$I_i^\pi \to I_f^\pi$	$B(E2)$	$J_i^\pi \to J_f^\pi$	$B(E2)$	$cB(E2)$	$\Delta(\%)$
$2_1^+ \to 0_1^+$	63.60	$3/2_1^+ \to 1/2_1^+$	57.00	57.00	−10.38
		$5/2_1^+ \to 1/2_1^+$	57.06	57.06	−10.28
$4_1^+ \to 2_1^+$	103.59	$7/2_1^+ \to 3/2_1^+$	92.14	102.38	−1.17
		$7/2_1^+ \to 5/2_1^+$	10.22	102.24	−1.30
		$9/2_1^+ \to 5/2_1^+$	102.36	102.36	−1.19

the energy of the first 4^+ state to that of the first 2^+ state, $R_{4/2} = E(4^+)/E(2^+)$, the addition of a Λ particle alters it from 3.083 to 2.829 with the PC-F1 parameter set. Here, the ratio for the hypernucleus is estimated as $E(9/2_1^+)/E(5/2_1^+)$. The $R_{4/2}$ ratio for the core nucleus is close to the value for a rigid rotor; that is, $R_{4/2} = 3.33$. On the other hand, the $R_{4/2}$ ratio is significantly reduced in the hypernucleus. It is in between the rigid-rotor limit and the vibrator limit; that is, $R_{4/2} = 2.0$, even though the $R_{4/2}$ ratio is still somewhat closer to the rigid-rotor value. This indicates a signature of disappearance of deformation found in the previous mean-field calculations [12], even though the deformation does not seem to disappear completely and thus the spectrum still shows a rotational-like character. Of course, the weaker polarization effect of a Λ particle, which has been found also in Ref. [35], compared with that in the previous mean-field calculations is due to the beyond-mean-field effect; that is, a combination of the effect of shape fluctuation and the angular-momentum projection. In particular, the GCM calculations for the core nucleus indicate that the average deformation depends on the angular momentum (see Fig. 1). The impact of the Λ particle may therefore be state dependent as well.

The calculated quadrupole transition strengths, $B(E2)$, are listed in Table I. Here we also show the $cB(E2)$ values, which are defined as [38]

$$cB(E2:I_i \to I_f) \equiv \frac{1}{(2I_i+1)(2J_f+1)} \begin{Bmatrix} I_f & J_f & j_\Lambda \\ J_i & I_i & 2 \end{Bmatrix}^{-2} \times B(E2:J_i \to J_f), \tag{9}$$

where I_i and I_f are the dominant angular momenta of the core nucleus in the initial and the final hypernuclear configurations, while j_Λ is that for the Λ particle. In the transitions shown in Table I, j_Λ is $1/2$. This equation is derived by relating

$$B(E2:J_i \to J_f) = \frac{1}{2J_i+1} |\langle J_i || \hat{T}_{E2} || J_f \rangle|^2 \tag{10}$$

$$\sim \frac{1}{2J_i+1} |\langle [j_\Lambda \otimes I_i]^{(J_i)} || \hat{T}_{E2} || \times [j_\Lambda \otimes I_f]^{(J_f)} \rangle|^2, \tag{11}$$

with

$$B(E2: I_i \to I_f) = \frac{1}{2I_i + 1} |\langle I_i || \hat{T}_{\rm E2} || I_f \rangle|^2, \qquad (12)$$

where $\hat{T}_{\rm E2}$ is the $E2$ transition operator (which acts only on the core states). The table indicates that the $B(E2)$ transition strengths decrease by adding a Λ particle into the core nucleus. This is consistent with the reduction in deformation in the hypernucleus as discussed in the previous paragraph.

IV. SUMMARY

We have investigated the role of beyond-mean-field effects on the deformation of $^{31}_{\Lambda}$Si. For this hypernucleus, the previous study based on the relativistic mean-field theory had shown that the deformation vanishes while the core nucleus ^{30}Si is oblately deformed. By using the microscopic particle-rotor model, we have shown that the ratio of the energy of the first 4^+ state to that of the first 2^+ state is significantly reduced by adding a Λ particle to ^{30}Si, even though the spectrum of the hypernucleus $^{31}_{\Lambda}$Si still shows a rotational-like structure. This implies that the addition of a Λ particle to ^{30}Si does not lead to a complete disappearance of nuclear deformation if the beyond-mean-field effect is taken into account, even though the deformation is indeed reduced to some extent. In accordance with this, the quadrupole transition strengths have been found to be also reduced in the hypernucleus.

Our study in this paper clearly shows that the beyond-mean-field effect plays an important role in the structure of hypernuclei. We emphasize that the microscopic particle-rotor model employed in this paper provides a convenient tool for that purpose, which is complementary to the generator coordinate method for the whole core + Λ-particle system [32].

ACKNOWLEDGMENTS

We thank H. Tamura for useful discussions. This work was supported in part by JSPS KAKENHI Grant No. 2640263 and by the National Natural Science Foundation of China under Grant No. 11575148.

[1] A. Bohr and B. R. Mottelson, *Nuclear Structure* (Benjamin, Reading, 1975), Vol. II.
[2] P. Ring and P. Schuck, *The Nuclear Many-Body Problem* (Springer-Verlag, New York, 1980).
[3] M. Bender, P.-H. Heenen, and P.-G. Reinhard, Rev. Mod. Phys. **75**, 121 (2003).
[4] T. Dytrych, K. D. Launey, J. P. Draayer, P. Maris, J. P. Vary, E. Saule, U. Catalyurek, M. Sosonkina, D. Langr, and M. A. Caprio, Phys. Rev. Lett. **111**, 252501 (2013).
[5] P. Maris, M. A. Caprio, and J. P. Vary, Phys. Rev. C **91**, 014310 (2015).
[6] S. R. Stroberg, H. Hergert, J. D. Holt, S. K. Bogner, and A. Schwenk, Phys. Rev. C **93**, 051301(R) (2016).
[7] G. R. Jansen, M. D. Schuster, A. Signoracci, G. Hagen, and P. Navratil, Phys. Rev. C **94**, 011301 (2016).
[8] C. N. Gilbreth, Y. Alhassid, and G. F. Bertsch, Phys. Rev. C **97**, 014315 (2018).
[9] H. Feshbach, in *Proceedings of the Summer Study Meeting on K-Physics and Facilities, Brookhaven, 1976*, edited by B. Palevsky (Brookhaven National Laboratory Report No. BNL-50579, 1976), p. 391.
[10] J. Žofka, Czech. J. Phys. **B30**, 95 (1980).
[11] X. R. Zhou, H.-J. Schulze, H. Sagawa, C. X. Wu, and E.-G. Zhao, Phys. Rev. C **76**, 034312 (2007).
[12] M. Thi Win and K. Hagino, Phys. Rev. C **78**, 054311 (2008).
[13] H.-J. Schulze, M. Thi Win, K. Hagino, and H. Sagawa, Prog. Theor. Phys. **123**, 569 (2010).
[14] B.-N. Lu, E.-G. Zhao, and S.-G. Zhou, Phys. Rev. C **84**, 014328 (2011).
[15] M. Isaka, M. Kimura, A. Dote, and A. Ohnishi, Phys. Rev. C **83**, 044323 (2011).
[16] M. Thi Win, K. Hagino, and T. Koike, Phys. Rev. C **83**, 014301 (2011).
[17] M. Isaka, H. Homma, M. Kimura, A. Dote, and A. Ohnishi, Phys. Rev. C **85**, 034303 (2012).
[18] M. Isaka, M. Kimura, A. Dote, and A. Ohnishi, Phys. Rev. C **87**, 021304 (2013).
[19] M. Isaka, K. Fukukawa, M. Kimura, E. Hiyama, H. Sagawa, and Y. Yamamoto, Phys. Rev. C **89**, 024310 (2014).
[20] B.-N. Lu, E. Hiyama, H. Sagawa, and S.-G. Zhou, Phys. Rev. C **89**, 044307 (2014).
[21] J.-W. Cui, X.-R. Zhou, and H.-J. Schulze, Phys. Rev. C **91**, 054306 (2015).
[22] O. Hashimoto and H. Tamura, Prog. Part. Nucl. Phys. **57**, 564 (2006).
[23] K. Hagino and J. M. Yao, in *Relativistic Density Functional for Nuclear Structure*, edited by J. Meng, Int. Rev. Nucl. Phys. 10 (World Scientific, Singapore, 2016), p. 263.
[24] A. Gal, E. V. Hungerford, and D. J. Millener, Rev. Mod. Phys. **88**, 035004 (2016).
[25] M. Bender and P.-H. Heenen, Phys. Rev. C **78**, 024309 (2008).
[26] T. R. Rodriguez and J. L. Egido, Phys. Rev. C **81**, 064323 (2010).
[27] J. M. Yao, J. Meng, P. Ring, and D. Vretenar, Phys. Rev. C **81**, 044311 (2010).
[28] J. M. Yao, H. Mei, H. Chen, J. Meng, P. Ring, and D. Vretenar, Phys. Rev. C **83**, 014308 (2011).
[29] J. M. Yao, K. Hagino, Z. P. Li, J. Meng, and P. Ring, Phys. Rev. C **89**, 054306 (2014).
[30] B. Bally, B. Avez, M. Bender, and P.-H. Heenen, Phys. Rev. Lett. **113**, 162501 (2014).
[31] J. L. Egido, M. Borrajo, and T. R. Rodriguez, Phys. Rev. Lett. **116**, 052502 (2016).
[32] H. Mei, K. Hagino, and J. M. Yao, Phys. Rev. C **93**, 011301(R) (2016).
[33] X. Y. Wu, H. Mei, J. M. Yao, and X.-R. Zhou, Phys. Rev. C **95**, 034309 (2017).
[34] J.-W. Cui, X.-R. Zhou, L.-X. Guo, and H.-J. Schulze, Phys. Rev. C **95**, 024323 (2017).
[35] M. Isaka, Y. Yamamoto, and Th. A. Rijken, Phys. Rev. C **94**, 044310 (2016).
[36] H. Mei, K. Hagino, J. M. Yao, and T. Motoba, Phys. Rev. C **90**, 064302 (2014).

[37] W. X. Xue, J. M. Yao, K. Hagino, Z. P. Li, H. Mei, and Y. Tanimura, Phys. Rev. C **91**, 024327 (2015).
[38] H. Mei, K. Hagino, J. M. Yao, and T. Motoba, Phys. Rev. C **91**, 064305 (2015).
[39] H. Mei, K. Hagino, J. M. Yao, and T. Motoba, Phys. Rev. C **93**, 044307 (2016).
[40] H. Mei, K. Hagino, J. M. Yao, and T. Motoba, Phys. Rev. C **96**, 014308 (2017).
[41] T. Bürvenich, D. G. Madland, J. A. Maruhn, and P.-G. Reinhard, Phys. Rev. C **65**, 044308 (2002).
[42] Y. Tanimura and K. Hagino, Phys. Rev. C **85**, 014306 (2012).
[43] P. W. Zhao, Z. P. Li, J. M. Yao, and J. Meng, Phys. Rev. C **82**, 054319 (2010).
[44] M. S. Basunia, Nucl. Data Sheets **111**, 2331 (2010); National Nuclear Data Center (NNDC), http://www.nndc.bnl.gov/.
[45] M. M. Sharma, M. A. Nagarajan, and P. Ring, Phys. Lett. B **312**, 377 (1993).
[46] P.-G. Reinhard, Z. Phys. A: At. Nucl. (1975) **285**, 93 (1978).